Anatomical features in children with orbital complications due to acute rhinosinusitis

Original Article

Authors

José Alberto Fernandes
Unidade Local de Saúde São João, Porto, Portugal

Patrícia Silva Sousa
Unidade Local de Saúde São João, Porto, Portugal

António Andrade
Unidade Local de Saúde São João, Porto, Portugal

Pedro Valente
Unidade Local de Saúde São João, Porto, Portugal

Ricardo Vaz
Unidade Local de Saúde São João, Porto, Portugal

Correspondence:
José Alberto Fernandes
zefernandes13@hotmail.com

Article received on June 16, 2025.
Accepted for publication on November 9, 2025.

Abstract

Objective: To investigate the relationship between anatomical landmarks identified by computed tomography (CT) and the severity of orbital complications of acute rhinosinusitis (ARS) in the pediatric population.

Materials and Methods: A retrospective study was conducted between 2012 and 2022 in children with a clinical and imaging diagnosis of complicated acute rhinosinusitis (ARS). Computed tomography (CT) scans of the paranasal sinuses were analyzed to assess the Lund-Mackay score, obstruction of the ostiomeatal complex (OMC), and the presence of anatomical landmarks (agger nasi, concha bullosa, infraorbital and Onodi cells, nasal septal deviation, inferior turbinate hypertrophy, and lamina papyracea dehiscence). Orbital complications were classified according to the Chandler scale.

Results: A total of 86 children were included. A significant difference was observed in the Lund-Mackay score between the side with the complication (mean: 6.3) and the contralateral side (mean: 4.7; $p < 0.001$). The coexistence of two or more anatomical landmarks on the affected side was significantly more frequent ($p < 0.01$). No isolated anatomical landmark showed a statistically significant association with clinical severity. The combination of agger nasi, infraorbital cells, and concha bullosa was correlated with increased severity of orbital complications (Chandler ≥ II; $p = 0.0431$).

Conclusion: The combined presence of specific anatomical landmarks — particularly agger nasi cells, infraorbital cells, and concha bullosa — is associated with more severe forms of orbital complications in children with acute rhinosinusitis (ARS). Detailed CT evaluation may be crucial for risk stratification and early definition of the therapeutic approach.

Keywords: Acute rhinosinusitis; orbital complications; nasal anatomy; anatomical landmarks; computed tomography; child

Introduction

Acute rhinosinusitis (ARS) is one of the most common infections in the pediatric population and is typically triggered by viruses affecting the upper respiratory tract. In 5–7% of cases, the disease may progress to orbital complications, which carry a substantial risk of morbidity[1-3]. These complications are facilitated by anatomical characteristics specific to children; specifically, the close proximity of the ethmoid sinuses to the orbit and thinness of the lamina papyracea allow direct spread of infection, while valveless venous drainage may enable retrograde propagation of inflammation[4–6].

Anatomic variants such as anterior ethmoid cells (agger nasi), concha bullosa, nasal septum deviation, and infraorbital ethmoid cells (Haller cells) can obstruct the ostiomeatal complex (OMC), causing mucus retention and persistent infection[7,8]. Although the anatomical factors involved in ARS are well described, few studies have systematically examined the association between nasal anatomical variants and severity of orbital complications in children with ARS.

Materials and Methods

We conducted a retrospective, observational, descriptive study at the Department of Otorhinolaryngology of the São João Local Health Unit between January 2012 and December 2022. The primary objective was to evaluate the association between nasal cavity anatomical variants and both the incidence and severity of orbital complications in pediatric ARS. The study included patients under 18 years of age who were hospitalized with a clinical and radiological diagnosis of ARS complicated by orbital involvement. The inclusion criterion was that the patient must have undergone a computed tomography (CT) scan of the paranasal sinuses during the acute episode. The exclusion criteria were orbital complications of noninfectious origin (traumatic, neoplastic, or inflammation due to other etiologies) and cases in which adequate imaging studies were unavailable. Imaging evaluation was performed by two otolaryngologists who were blinded to the side of the complication. Each CT scan was analyzed in the axial, coronal, and sagittal planes using bone and soft tissue windows. For each side, the following parameters were recorded:

- Lund-Mackay score (Table 1), which assesses opacification of the maxillary, frontal, anterior ethmoid, posterior ethmoid, and sphenoid sinuses, assigning 0–2 points to each sinus and the OMC, for a maximum total score of 24, according to the original description by *Lund* and *Mackay*[9].
- OMC obstruction was classified as obstructed or non-obstructed (Table 1).
- Presence and laterality of major nasal anatomical variants, including agger nasi cells, concha bullosa, infraorbital cells, Onodi cells, nasal septal deviation, inferior turbinate hypertrophy, and lamina papyracea dehiscence.

The severity of orbital complications was classified according to the Chandler scale (Table 2), which categorizes complications into five escalating grades: I – preseptal cellulitis, II – orbital cellulitis, III – subperiosteal abscess, IV – orbital abscess, and V – cavernous sinus thrombosis. For statistical analysis, complications were grouped into mild (grade I) and severe (grade II or higher).

Table 1
Lund-Mackay score

Paranasal sinuses
Maxillary (0,1,2)
Anterior ethmoid (0,1,2)
Posterior ethmoid (0,1,2)
Sphenoid (0,1,2)
Frontal (0,1,2)
OMC (0,2)*
Total
0 – No changes
1 – Partial opacification
2 – Total opacification
*0 – no obstruction, 2 – obstruction

OMC, ostiomeatal complex

Table 2
Chandler scale of orbital complications of ARS

Chandler scale
I (preseptal cellulite)
II (orbital cellulite)
III (subperiosteal abscess)
IV (orbital abscess)
V (cavernous sinus thrombosis)

ARS, acute rhinosinusitis

Statistical analysis was conducted using the IBM SPSS *Statistics*® software version 26.0 (IBM Corp., Armonk, NY, USA). Anatomical variants and the Lund-Mackay score were compared between the affected and contralateral sides using the McNemar's test for categorical variables and the Mann–Whitney U test for continuous variables, as the data were not normally distributed. Associations between combinations of anatomical variants and severity of orbital complications were analyzed using the Fisher's exact test due to the asymmetric distribution of categorical variables. A p-value < 0.05 was considered statistically significant.

Results

A total of 86 children diagnosed with ARS complicated by orbital involvement were evaluated. Their age ranged from 2 to 17 years, with a mean age of 9.2 years (standard deviation [SD] ± 3.1 years) and a slight male predominance (n = 46, 53%).

Regarding the severity of orbital complications, most cases (n = 68, 79%) were classified as Chandler grade II or higher. Specifically, 18 children (21%) had preseptal cellulitis (grade I), 35 (41%) had orbital cellulitis (grade II), 24 (28%) had subperiosteal abscess (grade III), seven (8%) had orbital abscess (grade IV), and two (2%) had cavernous sinus thrombosis (grade V). Imaging analysis revealed a statistically significant difference between the affected and contralateral sides in terms of the inflammatory disease extent (Table 3). More than half of the children exhibited complete opacification of the maxillary, ethmoid, and

Table 3
Comparison of Lund-Mackay scores for paranasal sinus opacification between the complicated and uncomplicated sides in children with ARS

		Side with Complication (n)	Side with complication (%)	Side without complication (n)	Side without complication (%)	p
Maxillary sinus	No changes	3	3.5%	20	23.3%	<0.001
	Partial opacification	7	8.1%	26	30.2%	
	Total opacification	76	88.4%	40	46.5%	
Anterior ethmoid	No changes	3	3.5%	25	29.1%	<0.001
	Partial opacification	7	8.1%	26	30.2%	
	Total opacification	76	88.4%	35	40.7%	
Posterior ethmoid	No changes	5	5.8%	18	20.9%	<0.001
	Partial opacification	8	9.3%	35	40.7%	
	Total opacification	73	84.9%	33	38.4%	
Frontal sinus	No changes	14	16.3%	23	26.7%	<0.001
	Partial opacification	8	9.3%	17	19.8%	
	Total opacification	64	74.4%	46	53.5%	
Sphenoid sinus	No changes	24	27.9%	43	50.0%	<0.001
	Partial opacification	45	52.3%	32	37.2%	
	Total opacification	17	19.8%	11	12.8%	

ARS, acute rhinosinusitis

frontal sinuses, along with partial opacification of the sphenoid sinus (Table 3). The mean Lund-Mackay score on the affected side was 6.3 ± 1.2, compared with 4.7 ± 2.3 on the unaffected side, demonstrating a statistically significant difference ($p < 0.001$). Similarly, OMC obstruction was identified in 92% of the sides with complications versus 46% of the contralateral sides (Table 4). Among the anatomical variants, agger nasi cells were the most frequent, present in the affected side in 44 children (51%). Nasal septal deviation toward the side of the complication was observed in 38 children (44%). Inferior turbinate hypertrophy was found in 35 children (41%), concha bullosa in 16 (19%), infraorbital cells in 12 (14%), and Onodi cells in seven children (8%). Lamina papyracea dehiscence was identified in seven children (8.1%), always ipsilateral to the complication (Table 4).

Table 4
Frequency of nasal anatomical variants and Lund-Mackay scores on the complicated and uncomplicated sides in children with ARS

		Side with Complication (n)	Side with complication (%)	Side without complication (n)	Side without complication (%)	p
OMC obstruction	-	7	8,1%	46	53,5%	<0,001
	+	79	91,9%	40	46,5%	
Septal deviation	-	48	55,8%	72	83,7%	<0,001
	+	38	44,2%	14	16,3%	
Agger nasi cells	-	42	48,8%	63	73,3%	0,332
	+	44	51,2%	23	26,7%	
Concha bullosa	-	70	81,4%	70	81,4%	1,000
	+	16	18,6%	16	18,6%	
Inferior turbinate hypertrophy	-	51	59,3%	66	76,7%	0,014
	+	35	40,7%	20	23,3%	
Infraorbital cells	-	74	86,0%	74	86,0%	1,000
	+	12	14,0%	12	14,0%	
Onodi cells	-	79	91,9%	79	91,9%	1,000
	+	7	8,1%	7	8,1%	
Lund-Mackay score		6,3 ± 1,2		4,7 ± 2,3		<0,001

ARS, acute rhinosinusitis; OMC, ostiomeatal complex

Table 5
Correlation between anatomical variants and orbital complications

Anatomical variants	Complication (Chandler)	n	%	p
Septal deviation	I	27	56.3%	0.104
	≥II	11	28.9%	
Agger nasi cells	I	20	45.5%	0.597
	≥II	22	54.5%	
Concha bullosa	I	9	56.3%	1.000
	≥II	7	43.7%	
Infraorbital cells	I	5	41.7%	0.728
	≥II	7	58.3%	

Figure 1
Association between anatomical variant combinations and severity of orbital complications

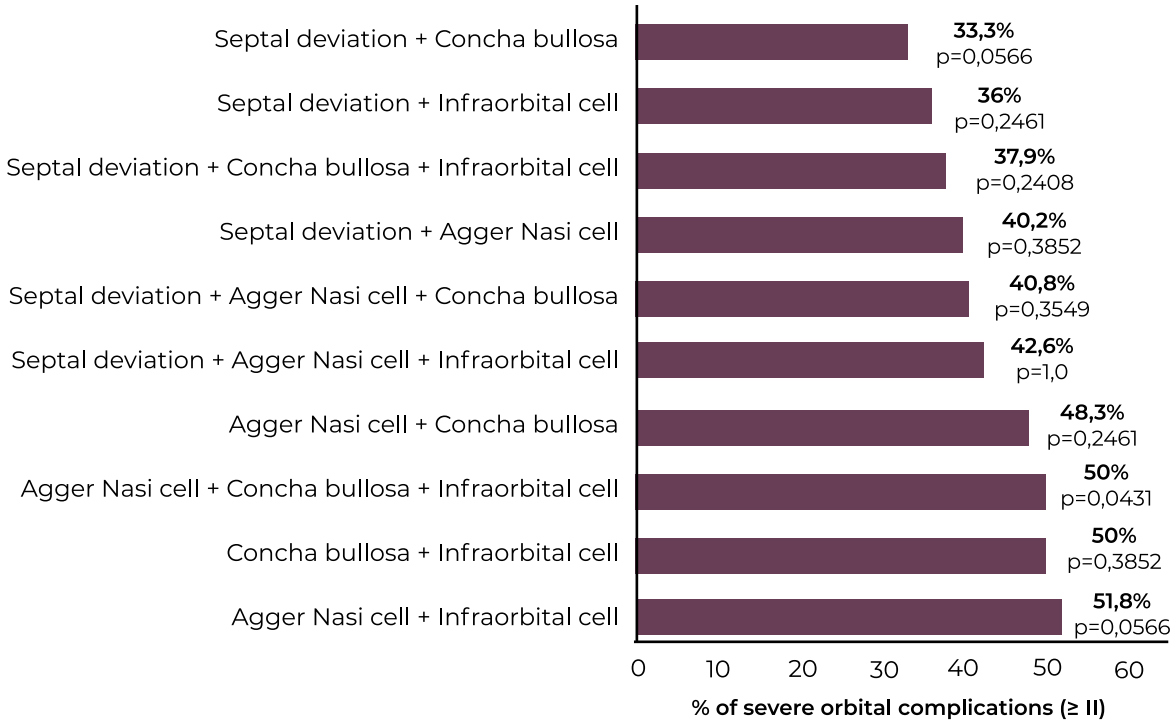

Notably, 61% patients had two or more anatomical variants on the affected side, compared with only 24% on the contralateral side, with a statistically significant difference ($p < 0.01$), suggesting an association between multiple variants and the side of the complication. Although several variants were common in the sample, none individually demonstrated a statistically significant association with the severity of orbital complications (Table 5). The combined presence of agger nasi cells, concha bullosa, and infraorbital cells was significantly associated with severe orbital complications (Chandler ≥ II) ($p = 0.0431$) (Figure 1).

Discussion

This study demonstrates a clear association between the presence of multiple nasal cavity anatomical variants and severity of orbital complications in children with ARS. The presence of a combination of agger nasi cells, infraorbital cells, and concha bullosa significantly correlated with more severe orbital involvement, reinforcing the role of local anatomy in disease pathogenesis. Previous studies have shown that variants affecting the morphology and diameter of the OMC impair sinus ventilation and drainage, promoting mucus stasis and bacterial proliferation. Bolger et al. and Fadda et al. reported associations between agger nasi cells or concha bullosa and mucosal opacification, and suggested impaired physiological drainage in the perinasal sinuses[7,8].

More recent studies have revealed that children with orbital complications secondary to ARS exhibit a higher prevalence of variants such as inferior turbinate hypertrophy and agger nasi cells on the affected side, consistent with our findings[10,11].

Recent perinasal CT-based studies have also highlighted the importance of assessing the lamina papyracea in patients with orbital complications[12]. In our study, lamina papyracea dehiscence was detected in 8% cases. Although infrequent, this variant is clinically relevant because the medial orbital wall is the most common site of direct extension of infection[13]. Hendy et al. reported that lamina

papyracea dehiscence had a prevalence of 1.1% in pediatric populations, and associated this variant with an increased risk of orbital abscess and need for surgical drainage[5].

No isolated variant showed a statistically significant association with the severity of orbital complications, consistent with the findings of Deniz and Tekinhatun, and Bedwell and Bauman, who highlighted the multifactorial nature of the infectious process, shaped not only by the local anatomy but also by the bacterial flora, disease duration, and immune response[12,14,15].

Onodi cells were identified in 8.1% cases but were not included in the analysis presented in Table 5. This methodological choice reflects their lack of direct influence on OMC patency, which is the main obstruction site involved in the pathophysiology of complicated ARS. Thus, their inclusion would not have statistical relevance in relation to the severity of orbital complications. Nevertheless, Onodi cells remain clinically relevant, particularly in surgical planning, due to their posterior sphenoethmoidal location and proximity to critical structures such as the optic nerve and internal carotid artery.

The limitations of this study include its retrospective design, absence of a control group with uncomplicated ARS, and sole reliance on CT without intraoperative confirmation. Selection bias is also possible, given the high prevalence of certain anatomical variants in the sample, such as agger nasi cells. Furthermore, sinus development varies across pediatric ages, which may influence the identification of these anatomical variants and their correlation with orbital complications. Despite these limitations, our findings align with current literature and highlight the clinical significance of the early identification of nasal anatomical variants.

CT evaluation of the nasal anatomy is particularly useful when clinical signs suggest orbital involvement. The coexistence of anatomical variants, particularly agger nasi cells, infraorbital cells, and concha bullosa, should be regarded as a clinical warning sign, prompting closer monitoring, early initiation of antibiotic therapy, or surgical intervention in selected cases.

Conclusion

This study demonstrates that the coexistence of anatomical variants, particularly agger nasi cells, infraorbital cells, and concha bullosa, is significantly associated with more severe orbital complications in children with ARS. Detailed CT assessment of the nasal anatomy is a valuable tool for risk stratification and therapeutic decision-making. Future prospective studies are needed to validate these findings and further define their clinical applicability.

Conflicts of interest

The authors declare that they have no conflict of interest regarding this article.

Data confidentiality

The authors declare that they followed the protocols of their work in publishing patient data.

Human and animal protection

The authors declare that the procedures followed are in accordance with the regulations established by the directors of the Commission for Clinical Research and Ethics and in accordance with the Declaration of Helsinki of the World Medical Association. Privacy policy, informed consent and Ethics committee authorisation. The authors declare that they have obtained signed consent from the participants and that they have local ethical approval to carry out this work.

Financial support

This work did not receive any grant contribution, funding or scholarship.

Scientific data availability

There are no publicly available datasets related to this work.

Declaration on the Use of Generative AI and AI-Assisted Technologies in the Writing Process

During the preparation of this work, the author used ChatGPT (OpenAI) exclusively to improve the language and readability of the text. The artificial intelligence tool did not replace any role of the authors in the conception, analysis, interpretation of data, or scientific writing of this article. After using the tool, the content was carefully reviewed and edited by the authors, who assume full responsibility for the content of the publication.

References

1. Chandler JR, Langenbrunner DJ, Stevens ER. The pathogenesis of orbital complications in acute sinusitis. Laryngoscope. 1970 Sep;80(9):1414-28. doi: 10.1288/00005537-197009000-00007.
2. Wald ER. Sinusitis in children. N Engl J Med. 1992 Jan 30;326(5):319-23. doi: 10.1056/NEJM199201303260507.
3. Hamilos DL. Chronic rhinosinusitis: epidemiology and medical management. J Allergy Clin Immunol. 2011 Oct;128(4):693-707; quiz 708-9. doi: 10.1016/j.jaci.2011.08.004
4. Som PM, Curtin HD. Head and Neck Imaging. 4ª ed. St. Louis: Mosby; 2003. Disponível em: https://www.worldcat.org/oclc/759159389
5. Hendy K, Taranath A, Ghabriel M, Nasserallah M. Lamina papyracea dehiscence CT incidence in paediatric population. Austin J Anat.[Internet] 2021;8(3):e1105. Available from: https://austinpublishinggroup.com/anatomy/fulltext/Anatomy-v8-id1105.pdf
6. Wan Y, Shi G, Wang H. Treatment of orbital complications following acute rhinosinusitis in children. Balkan Med J. 2016 Jul;33(4):401-6. doi: 10.5152/balkanmedj.2016.141065.
7. Bolger WE, Butzin CA, Parsons DS. Paranasal sinus bony anatomic variations and mucosal abnormalities: CT analysis. Laryngoscope. 1991 Jan;101(1 Pt 1):56-64. doi: 10.1288/00005537-199101000-00010.
8. Fadda GL, Rosso S, Aversa S, Petrelli A, Ondolo C, Succo G. Multiparametric statistical correlations between paranasal sinus anatomic variations and chronic rhinosinusitis. Acta Otorhinolaryngol Ital. 2012 Aug;32(4):244–51. Disponível em: https://pmc.ncbi.nlm.nih.gov/articles/PMC3468938/pdf/0392-100X-32-244.pdf
9. Lund VJ, Mackay IS. Staging in rhinosinusitis. Rhinology. 1993 Dec;31(4):183–4.
10. Çelik M, Kaya KH, Yegin Y, Olgun B, Kayhan FT. Anatomical factors in children with orbital complications due to acute rhinosinusitis. Iran J Otorhinolaryngol. 2019 Sep;31(106):289-295. Doi: 10.22038/ijorl.2019.35283.2161
11. Daniel A, Novoa R, Pansky I, Hazan I, Friedrich L, Kordeluk S. et al. The association between sinonasal anatomical variants and orbital complications in pediatric acute rhinosinusitis. Int J Pediatr Otorhinolaryngol. 2024 May:180:111958. doi: 10.1016/j.ijporl.2024.111958
12. Deniz MA, Tekinhatun M. Evaluation of lamina papyracea dehiscence with paranasal computed tomography. Eur Arch Otorhinolaryngol. 2024 Jul;281(7):3649-3654. doi: 10.1007/s00405-024-08538-8
13. Dankbaar JW, van Bemmel AJM, Pameijer FA. Imaging findings of the orbital and intracranial complications of acute bacterial rhinosinusitis. Insights Imaging. 2015 Oct;6(5):509-18. doi: 10.1007/s13244-015-0424-y.
14. Seltz LB, Smith J, Durairaj VD, Enzenauer RW, Todd J. Microbiology and antibiotic management of orbital cellulitis. Pediatrics. 2011 Mar;127(3):e566-72. doi: 10.1542/peds.2010-2117.
15. Bedwell JR, Bauman NM. Management of pediatric orbital cellulitis and abscess. Curr Opin Otolaryngol Head Neck Surg. 2011 Dec;19(6):467-73. doi: 10.1097/MOO.0b013e32834cd54a.